Amino Acids (2012) 43:937–949
DOI 10.1007/s00726-011-1154-1

ORIGINAL ARTICLE

Proliferation potential of human amniotic fluid stem cells differently responds to mercury and lead exposure

C. Gundacker · M. Scheinast · L. Damjanovic · C. Fuchs · M. Rosner · M. Hengstschläger

Received: 8 September 2011 / Accepted: 8 November 2011 / Published online: 19 November 2011

Abstract There are considerable gaps in our knowledge on cell biological effects induced by the heavy metals mercury (Hg) and lead (Pb). In the present study we aimed to explore the effects of these toxicants on proliferation and cell size of primary human amniotic fluid stem (AFS) cells. Monoclonal human AFS cells were incubated with three dosages of Hg and Pb (single and combined treatment; ranging from physiological to cytotoxic concentrations) and the intracellular Hg and Pb concentrations were analyzed, respectively. At different days of incubation the effects of Hg and Pb on proliferation, cell size, apoptosis, and expression of cyclins and the cyclin-dependent kinase inhibitor p27 were investigated. Whereas we found Hg to trigger pronounced effects on proliferation of human AFS cells already at low concentrations, anti-proliferative effects of Pb could only be detected at high concentrations. Exposure to high dose of Hg induced pronounced down-regulation of cyclin A confirming the anti-proliferative effects observed for Hg. Co-exposure to Hg and Pb did not cause additive effects on proliferation and size of AFS cells, and on cyclin A expression. Our here presented data provide evidence that the different toxicological effects of Pb and Hg on primary human stem cells are due to different intracellular accumulation levels of these two toxicants. These findings allow new insights into the functional consequences of Pb and Hg for mammalian stem cells and into the cell biological behavior of AFS cells in response to toxicants.

C. Gundacker (✉) · M. Scheinast · L. Damjanovic · C. Fuchs · M. Rosner · M. Hengstschläger
Institute of Medical Genetics, Medical University of Vienna, Währinger Straße 10, 1090 Vienna, Austria
e-mail: claudia.gundacker@meduniwien.ac.at

Keywords Amniotic fluid stem cells · Cell size · Lead acetate · Methyl mercury · Proliferation · Cyclin A

Introduction

The heavy metals mercury (Hg) and lead (Pb) are ubiquitous environmental pollutants. The general population is primarily exposed through ingestion of contaminated food and inhalation of contaminated air (Clarkson 2002; EFSA 2010). Pb and Hg (particularly methyl mercury—MeHg—an organic mercury compound) are well-known toxicants targeting the central nervous system. Both metals adversely affect kidney function, the immune system, and reproduction. Pb also affects hem synthesis. The underlying cytotoxic mechanisms include metal-induced oxidative stress, depletion of glutathione, disturbance of intracellular calcium, interference with cell signaling, necrotic and apoptotic cell death, and inhibition of cell cycle progression (Quig 1998; ATSDR 1999; Miura 2000; Rice and Barone 2000; Faustman et al. 2002; Clarkson et al. 2003; Papanikolaou et al. 2005; ATSDR 2007; Li et al. 2007).

The toxicity of Hg and Pb clearly manifests at high concentration levels. This is known from studies on occupationally exposed individuals and from mass intoxications. Additionally, in in vitro experiments usually very high amounts of Hg and Pb in micromolar (μM) range are applied to ensure that toxic mechanisms can be detected and investigated. Thus dose–response relationships are much better known for the high concentration ranges. However, Hg and Pb blood contents of non-occupationally and non-accidentally exposed humans are considerably lower—below 5 μg/L (0.025 μM) and below 200 μg/L (1 μM), respectively. Humans are frequently co-exposed to Hg and Pb via consumption of contaminated food and tap

water and by inhalation of contaminated air. The same is true for fetuses. Both metals trespass the placenta as well as the blood brain barrier (Goyer 1990; Stern and Smith 2003). It has been shown that neurological development can be impaired, when exposure to Hg and Pb is occurring during prenatal period and childhood (Wigle and Lanphear 2005; Grandjean and Landrigan 2006).

Human amniotic fluid stem (AFS) cells are of fetal origin. These pluripotent cells can form embryoid bodies and differentiate into cells of all three embryonic germ layers. AFS cells are regarded as an intermediate stage between embryonic stem cells and lineage-restricted adult progenitor cells and have many advantages over embryonic stem cells (e.g., tumor development and ethics) and adult stem cells (e.g., low proliferation rate and lineage-restricted potential). Due to their potential to differentiate into many different cell types, including neuronal cells (Rosner et al. 2011), monoclonal primary human AFS cells are an excellent model to study the cell biological effects of mercury and lead toxicity.

Despite the remarkable shortcomings in our knowledge on low-dose and co-exposure effects induced by Hg and Pb, these issues are seldom addressed. In the present study we thus aimed to explore the effects of Hg and Pb on proliferation and cell size of human AFS cells. For this purpose we treated the stem cells with three dosages (single and combined treatment) ranging from physiological to cytotoxic concentrations (0.03–3 μM of MeHg, 1–50 μM of lead acetate (PbAc)). In the here presented study we show that MeHg and PbAc treatment affects proliferation and cell size of human AFS cells in a dose-dependent manner and in relation to the amount of Hg and Pb accumulated in cells. We further show that MeHg interferes with cell cycle progression accompanied by downregulation of cyclin A. Combined exposure to these metals does not have additive effects on cell proliferation and cyclin A expression. These findings are of relevance for a better understanding of both, the toxic effects of Hg and Pb and the cell biological behavior of human AFS cells.

Materials and methods

Cell culture and reagents

Monoclonal human AFS cells (Q1; kindly provided by A. Atala, Wake Forest University School of Medicine) were cultivated at 37°C and 5% CO_2 in Chang C/MEMα medium 1:5 (Chang Medium C, Irvine Scientific, cat. no. T101-019; Minimal Essential Medium (MEM) α, Invitrogen, cat. no. 41061-029) supplemented with 15% fetal bovine serum (Hyclone, cat. no. HY-ME-SH30070.03), 2 mM L-Glutamine (PAA, M11-004), Penicillin (30 mg/L), and Streptomycin (50 mg/L).

Mercury and lead treatments

We examined the effects of MeHg and PbAc treatment on AFS cell proliferation and cell size, as well as the intracellular Hg and Pb accumulation on day 0 to day 4. Cells were seeded in six-well-plates and exposed on day 0 (i.e., about 20 h after seeding) to the metal compounds in different dosages (MeHg: 0.03, 0.3 and 3 μM; PbAc: 1, 10 and 50 μM; MeHg + PbAc: 0.03 μM MeHg + 1 μM PbAc, 0.3 μM MeHg + 10 μM PbAc, 3 μM MeHg + 50 μM PbAc). Stock solutions were prepared with MeHg chloride (Sigma-Aldrich) and Pb(II) acetate trihydrate (Merck). The salts were accurately dissolved and properly diluted in DMSO to achieve solutions with 30, 300, and 3,000 μM MeHg and with 1, 10, and 50 mM Pb. Two microlitre of stock solution were directly added to 2 mL cell growth media thereby diluted to a thousandth. We checked full solubilization of the salts by measuring Hg and Pb contents in medium two times and found values of 0.028 ± 0.008 (0.03 μM MeHg), 0.30 ± 0.07(0.3 μM MeHg), 3.00 ± 0.08 (3 μM MeHg), 1.1 ± 0.1 (1 μM Pb), 10.2 ± 0.2 (10 μM Pb), and 56 ± 5 (50 μM Pb). For control Q1 cells were treated with DMSO (double dose in co-exposure experiments). The proliferation experiment was made in triplicates. Q1 cells were harvested on day 0, 2, 3, and 4. Aliquots of each cell suspension were taken for analyses of cell number and cell size. For subsequent Hg and Pb analyses in Q1 cells, cells were pooled from triplicates. The cell suspension was divided into halves, centrifuged, and pellets were stored at −20°C until further analysis. Several further proliferation experiments were conducted to exactly determine effects of MeHg and PbAc treatment (single and combined exposure) on cell number and cell size of Q1 cells, and furthermore to examine effects on day 6. The experiments were conducted as described above and made in duplicates or triplicates.

Analysis of cell number and cell size

Cell number (number of vital cells after live/dead discrimination) and cell size (mean diameter of vital cells) were measured on a CASY cell counter and analyzer (Schärfe Systems, Innovatis, Reutlingen, Germany) on day 0 (prior to mercury and lead treatment) and after harvesting on days 2, 3, 4, and 6.

Cytofluorometric determination of fragmented DNA (subG1 content)

Q1 cells were cultivated as described above. They were seeded in 60 mm plates in triplicate and harvested on day 2, day 4, and day 6. Cells were fixed by rapid submersion in ice-cold 85% ethanol. DNA was stained with 0.25 mg/mL

propidium iodide, 0.05 mg/mL RNase, 0.1% Triton X-100 in citrate buffer, pH 7.8, and analyzed on a Beckton Dickinson FACSCALIBUR (Becton–Dickinson, San Jose, CA, USA) (Valli et al. 2010).

Protein extraction and immunoblotting

Q1 cells were cultivated as described above. The cells grew in 60 mm plates and were exposed on day 0 to MeHg (0.3, 3 μM), Pb Ac (10, 50 μM), and MeHg + PbAc (0.3 + 10, 3 + 50 μM) and harvested on day 4. Extracts of cellular total protein were prepared by physical disruption of cell membranes by repeated freeze&thaw cycles. Briefly, cells were washed with PBS and harvested by trypsinization. Pellets were washed twice with ice-cold PBS and lysed in buffer A containing 20 mM Hepes, pH 7.9, 0.4 M NaCl, 25% glycerol, 1 mM EDTA, 0.5 mM DTT, 1 mM PMSF, 0.5 mM NaF, 0.5 mM Na_3VO_4 supplemented with 2 μg/mL aprotinin, 2 μg/mL leupeptin, 0.3 μg/mL benzamidinchlorid, 10 μg/mL trypsininhibitor by freezing and thawing. Supernatants were collected by centrifugation at 20,000×*g* for 20 min at 4°C and stored at −80°C. Proteins were resolved by 11% SDS-PAGE and transferred to nitrocellulose. Blots were stained with Ponceau-S to visualize the amount of loaded protein. For immunodetection antibodies specific for the following proteins were used: cyclin D1 M-20 (Santa Cruz, #sc-718), cyclin A H-432 (Santa Cruz, #sc-751), $p27^{Kip1}$ clone 57 (Becton–Dickinson/Transduction Laboratories, #610241), and GAPDH, glyceraldehyde-3-phosphate dehydrogenase (Trevigen, #2275-PC-100). Rabbit polyclonal antibodies and mouse monoclonal antibodies were detected using anti-rabbit IgG, a HRP-linked heavy and light chain antibody from goat (A120-101P, Bethyl Laboratories) and anti-mouse IgG, a HRP-linked heavy and light chain antibody from goat (A90-116P, Bethyl Laboratories), respectively. Signals were visualized using the enhanced chemiluminescence method (Pierce).

Mercury and lead analyses

Thawed cell pellets were digested with a mixture of 2 mL 65 vol% HNO_3 (Merck, Suprapur) and 0.75 mL 30% H_2O_2 (Merck, p.a.) in pressurized Teflon vessels in a microwave digestion unit (MLS, mls 1200 mega). Sample solutions were volumetrically filled up with Millipore water to 10 mL. Hg concentrations were determined by cold vapor-AAS (CV-AAS), using a Hitachi Z 8200 Polarized Zeeman Atomic Absorption Spectrophotometer in combination with an amalgamation unit (Uwe Binninger Analytik, Germany) and a hydride generation system (Hitachi; HFS-3). Pb concentrations were analyzed with ET-AAS (graphite furnace). Quality assurance was achieved by measuring blank test solutions and reference materials (Seronorm Trace Elements Human Whole Blood L-2, 210205, LOT 1003192). Hg and Pb levels in reference material (14.8 ± 2.6 and 346 ± 45 μg/L; $N = 5$, respectively) remained well within the certified levels ranging between 13.6 and 16.8 μg/L for Hg and between 300 and 372 μg/L for Pb. The limit of detection was determined by the concentration equivalent to the threefold standard deviation of the signal of the blank solution and was 0.24 μg/L (Hg) and 0.30 μg/L (Pb). All metal contents were measured in duplicate by the working curve method.

Statistics

All results on cell number, cell size, and subG1 DNA content represent means ± SD for three or two data points except the Hg-induced effects on cell number on day 6 (Fig. 3a), which result from one single experiment. Hg and Pb concentrations represent means ± SD for two data points. Two group comparisons were made with *t* test using the SPSS 18.0 program (SPSS Inc, Chicago, IL). The tests were performed two-sided at $P < 0.05$.

Results and discussion

Effects of MeHg on cell number and cell size of AFS cells

For the exploration of low-dose and co-exposure effects in human AFS cells we chose concentrations ranging from physiological up to cytotoxic levels, i.e., 0.03, 0.3, and 3 μM MeHg and 1, 10, and 50 μM PbAc. The doses and compounds were selected on the basis of previous reports. Support for low-dose effects comes from studies reporting diminished proliferation/viability of rodent cells at concentrations as low as 0.03 μM (6 μg/L) MeHg and 0.5–1 μM (100–200 μg/L) Pb, which was primarily applied as PbAc (Chen et al. 2003; Sakaue et al. 2005; Tamm et al. 2006; Li et al. 2007). Numerous other studies demonstrated that cell proliferation and/or cell viability becomes increasingly reduced at about fivefold to tenfold higher concentration and beyond (e.g., Gribble et al. 2005; Corbit et al. 2006; Glahn et al. 2008; Agarwal et al. 2009).

Exposure of human AFS cells to 3 μM MeHg leads to markedly and progressively reduced proliferation. The mean cell number is reduced to 45 ± 8% on day 2, to 27 ± 5% on day 4, and to 12 ± 2% on day 6 (Figs. 1, 2, 3). The highly significant effects ($P < 0.001$) are also clearly visible in microscope pictures (Fig. 1a). To investigate whether apoptosis is involved in MeHg-induced reduction of AFS cell proliferation, we evaluated amount of cells with fragmented DNA (subG1 DNA content), which is

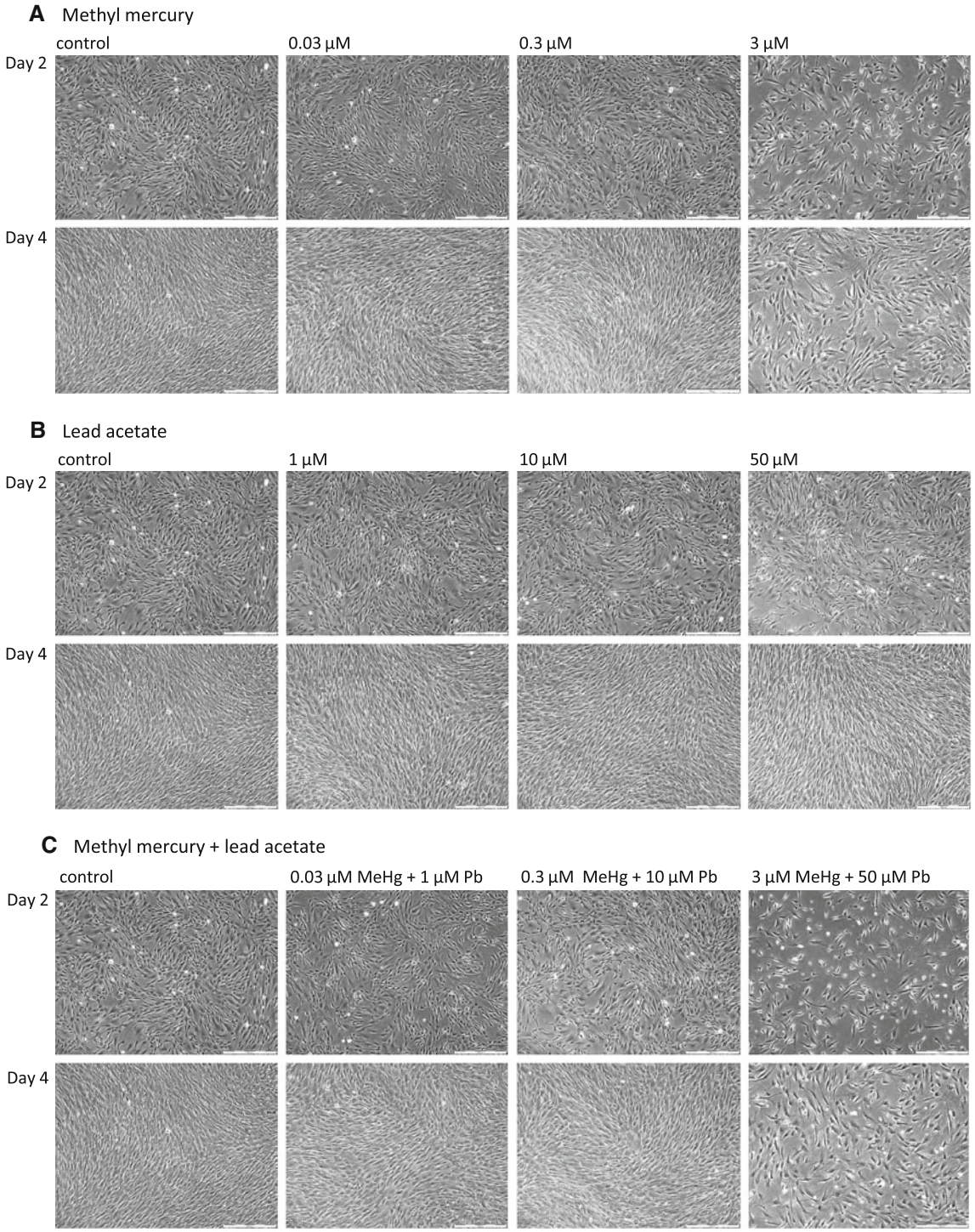

Fig. 1 Microscope pictures (4×) of human AFS cells Q1 on day 2 and day 4 (*scale bar*, 250 µM). Cells were treated on day 0 with (**a**) methyl mercury (MeHg), (**b**) lead acetate (PbAc), and (**c**) both MeHg and PbAc at different concentrations as indicated. Each set of presented data is derived from one single experiment

representative for the level of apoptosis. The subG1 DNA content of cells exposed to 0.03 and 0.3 µM MeHg does not differ from controls, whereas cells exposed to 3 µM show significantly higher subG1 DNA content compared with controls on days 2, 4, and 6 ($P < 0.05$, respectively) (Fig. 4). This finding indeed speaks for apoptotic effects induced by 3 µM MeHg regarding the significant decrease in cell number during this time (Fig. 2a). However, it is obvious that the dramatic anti-proliferative effects of 3 µM MeHg on AFS cells can clearly not be exclusively

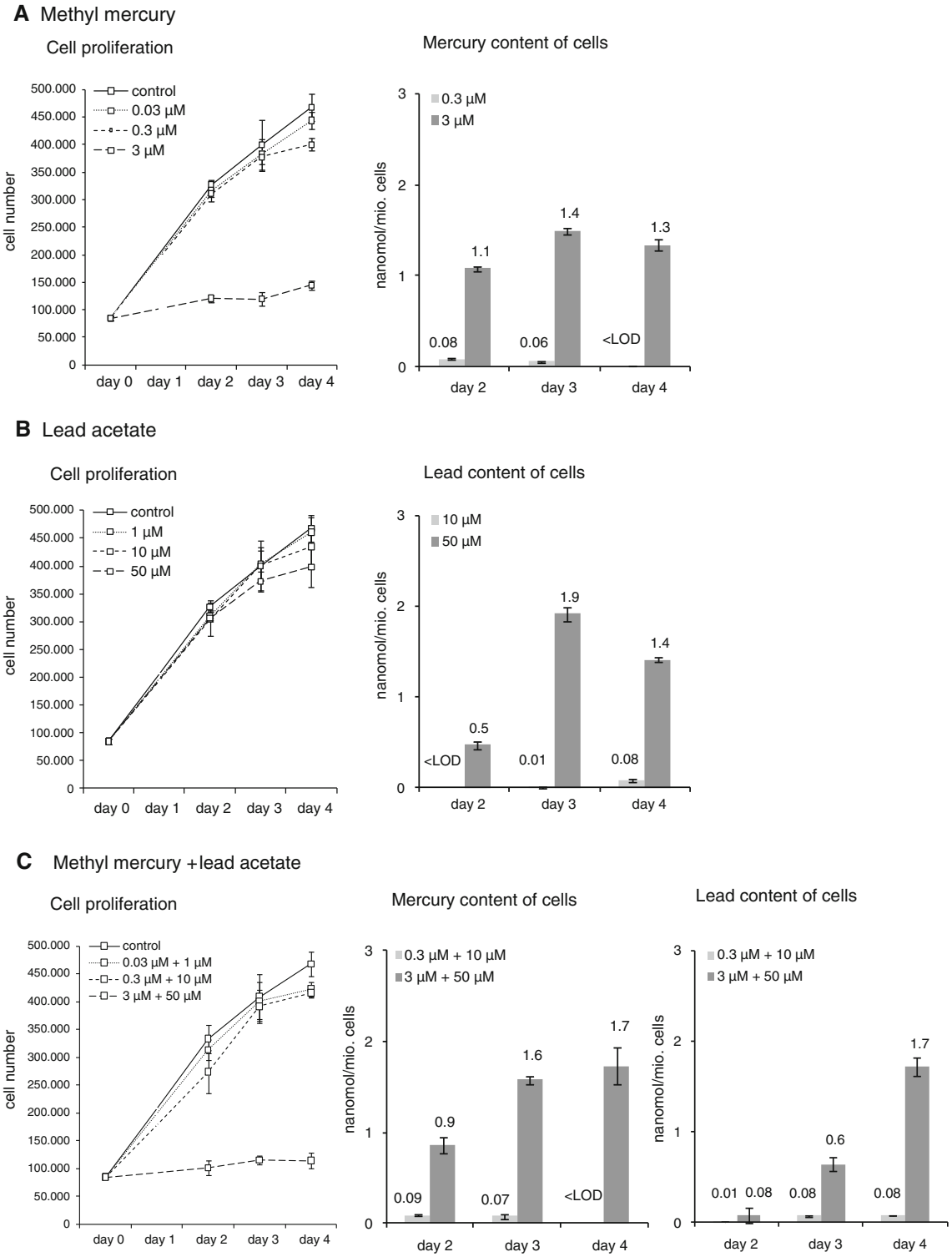

Fig. 2 *Left panel*: proliferation analyses of Q1 cells on day 0 to day 4. Cells were treated on day 0 with (**a**) MeHg, (**b**) PbAc, and (**c**) both MeHg and PbAc at different concentrations as indicated. Values are means ± SD of three data points. *Right panel*: Intracellular Hg and Pb contents in Q1 AFS cells on day 2, day 3, and day 4. Values are means ± SD of two data points. Hg and Pb concentrations in cells treated with 0.03 µM MeHg and 1 µM Pb (single and combined exposure) were <LOD and are not displayed. Each set of presented data is derived from one single experiment

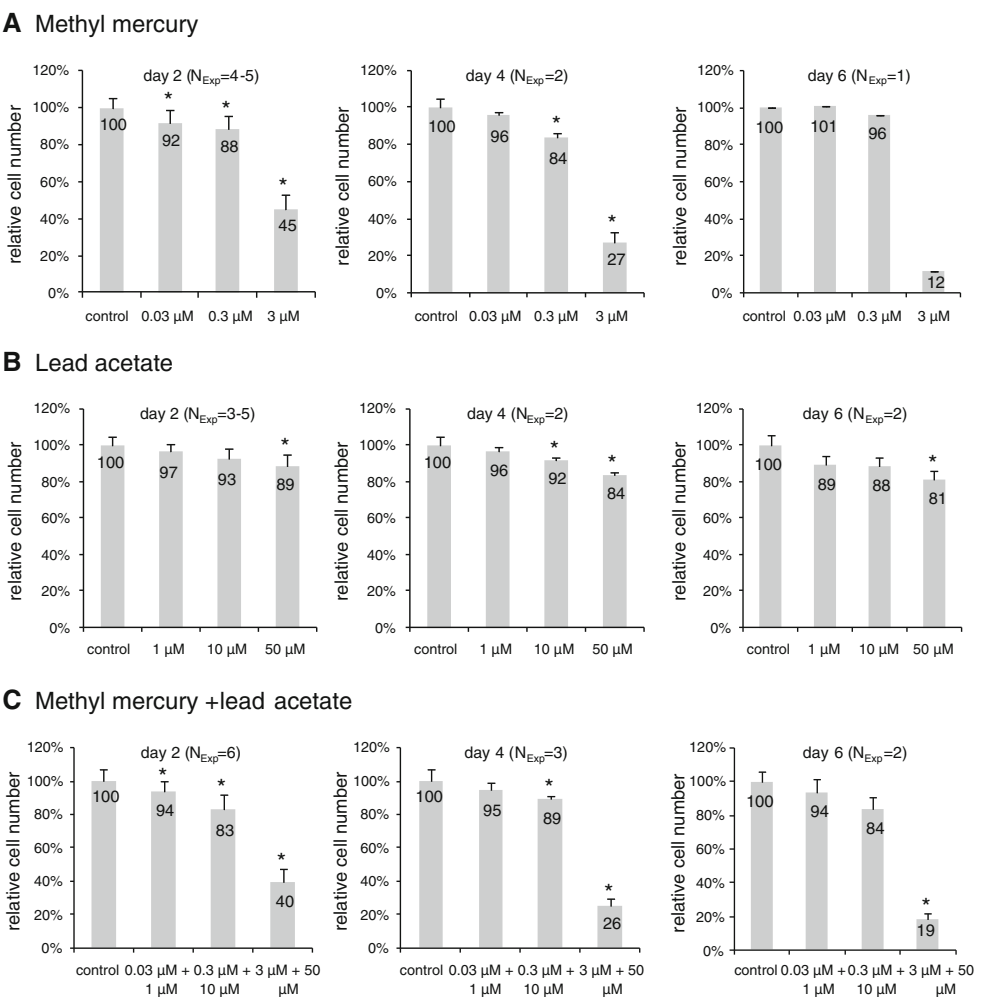

Fig. 3 Long-term effects of (**a**) MeHg, (**b**) PbAc, and (**c**) both MeHg and PbAc on human AFS cell number including day 6 analyses. Values are means ± SD of two or more independent experiments except the MeHg experiment on day 6. *Asterisks mark* significant differences between controls and metal-treated cells (*$P < 0.05$)

explained by the slight increase in apoptotic events at this time point (compare day 2 in Fig. 2a and in Fig. 4).

One of the major mechanisms of MeHg-induced apoptotic cell death is the metal-induced oxidative stress producing reactive oxygen species (ROS), which induces mitochondria-dependent apoptotic effects including increased DNA fragmentation, mitochondrial dysfunctions, activation of PARP and caspase cascades, enhanced pro-apoptotic proteins (Bax, Bad) and decreased Bcl-xL/Bcl-xS ratio, and activation of ERK1/2 and p38. In further studies, it was shown that besides caspases other cysteine proteases, the calpains, are concomitantly activated in MeHg-induced apoptosis. Calpain activation is preceded by perturbation of Ca^{2+} homeostasis (Sakaue et al. 2005; Tamm et al. 2006; Cuello et al. 2010; Lu et al. 2011; Pal et al. 2011). In MeHg-exposed cells apoptosis has also been reported to coexist with necrosis (necrosis might even predominate over apoptosis in dependence of exposure time; Cuello et al. 2010).

The fact, described above, that the observed stop of proliferation on day 2 upon treatment with 3 µM MeHg (Fig. 2a) cannot fully be explained by increased apoptosis (Fig. 4), argues that this toxicant also effects cell cycle regulation. In order to confirm this hypothesis we measured protein expression of cyclin D1, cyclin A, and the cyclin-dependent kinase inhibitor p27 via conventional SDS-Page, and Immunoblotting. We observed pronounced downregulation of cyclin A expression, whereas cyclin D1 is slightly upregulated in AFS cells exposed to 3 µM MeHg (single and combined exposure). Moreover, p27 expression appears to be unaffected by MeHg and PbAc exposures (Fig. 5). Neuronal precursor cells show unchanged p27 as well as unchanged or decreased cyclin D1 levels upon MeHg exposure (Burke et al. 2006; Falluel-Morel et al. 2007; Xu et al. 2010). The here observed pronounced effect of MeHg on cyclin A expression could be explained by MeHg-induced cell cycle arrest and stop of proliferation (further confirming effects described in proliferation experiments above) or by functional interaction between MeHg and cyclin A. In experiments with conditional knockout mice lacking both A-type cyclins it was found that cyclin A is essential for proliferation and colony formation of embryonic stem cells and hematopoietic stem

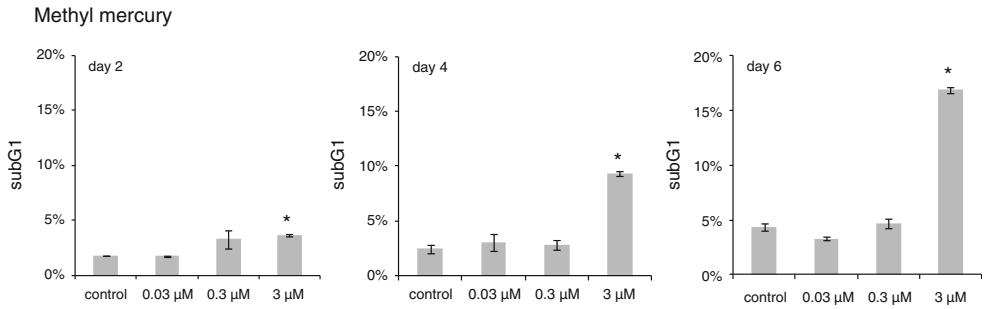

Fig. 4 Apoptosis analysis in Hg-treated human AFS cells. The relative amounts of cells with subG1 DNA content were cytofluorometrically analyzed at the indicated concentrations and time points. Values are means ± SD of triplicates. *Asterisks mark* significant differences between controls and MeHg-treated cells (*$P < 0.05$)

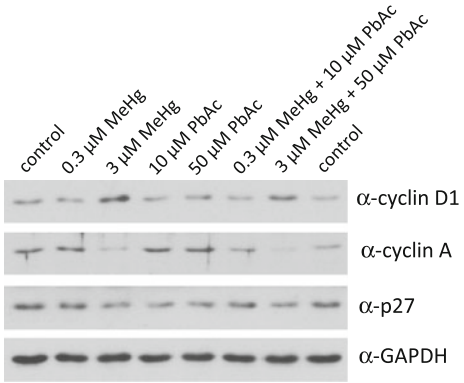

Fig. 5 Effects of MeHg and PbAc on expression of cyclin D1, cyclin A, and p27. Total protein lysates were prepared from human AFS cells exposed to MeHg and PbAc (single and combined exposure) until day 4, and analyzed via immunoblotting using indicated antibodies. GAPDH was used as protein loading control

cells but not fibroblast cells. It has been suggested that wiring of cell cycle pathways in stem cells may operate in a more rigid fashion than in other cell types. Furthermore, this mechanism may allow stem cells to selectively respond to environmental cues by specifically upregulating a particular component of the cell cycle engine and to undergo self-renewal, asymmetric division, or cell differentiation (Kalaszczynska et al. 2009).

Experiments on mouse neuroblastoma cells, rat PC12 cells, and mouse glioma cells have already earlier suggested that MeHg harbors the potential to disrupt the mitotic apparatus (through specific inhibition of microtubule formation). This is accompanied by a G2/M arrest and induced apoptotic cell death in both neuronal and non-neuronal cells (Miura 2000). Other studies demonstrated a crucial role of p53 in this G2/M arrest. p53+/+ (mouse fibroblast) cells are more sensitive to MeHg-induced cytotoxicity, cell cycle inhibition, and induction of apoptosis, while p53−/− cells undergo less necrosis and less apoptosis following MeHg treatment. 2.5 µM MeHg completely stops proliferation in p53+/+ cells, while over 40% of p53−/− cells are still able to reach a next round of cell cycle. 1 and 2.5 µM MeHg cause time- and dose-dependent accumulation of cells in G2/M phase independent of p53 genotype; however, the magnitude of change is p53-dependent (Gribble et al. 2005).

In addition, p21 was also reported to play a role in MeHg-induced inhibition of cell cycle progression, wherein a higher fraction of metal-treated p21−/− cells still completes one cell cycle round compared with p21 +/+ and p21+/− cells. However, cells of all p21 genotypes accumulate in G2/M phase, which indicates more complex relationship between p21 and other proteins involved in MeHg-induced cell cycle regulation (Faustman et al. 2002). Interestingly, MeHg also reduces the levels of cyclin E, which is a critical promoter of G1/S progression regulated by p21. The decrease of a cell cycle promoter suggests that MeHg is able to target cell machinery also by controlling the G1/S transition (Burke et al. 2006; Xu et al. 2010). Because cyclin E has been linked to both G1/S regulation and apoptosis, it has been assumed that early cell cycle arrest and subsequent apoptosis are linked by a common molecular mechanism (Burke et al. 2006). Cell cycle inhibition is regarded to protect the cell from toxic insult (Gribble et al. 2005).

In our proliferation experiments we also recorded cell diameter (as a function of cell volume actually measured by the electronic cell counter) and found that mean size of vital AFS cells exposed to 3 µM MeHg increases significantly up to 112 ± 7% (day 2), 111 ± 4% (day 4), and 106 ± 3% (day 6) of controls. This is also the case in cells co-exposed to 3 µM MeHg and 50 µM PbAc. Also their size increases to 114 ± 7% (day 2), 112 ± 5% (day 4), and 113 ± 3% (day 6) in relation to controls ($P < 0.05$, respectively; data not shown). In mammalian cells cell size is deregulated when cell cycle progression is stopped (Fingar et al. 2002). The observed increase in cell size thus might indicate that 3 µM MeHg-treated AFS cells might exhibit a deregulated cell cycle control in our here presented experiments.

Exposure of AFS cells to 0.03 and 0.30 μM MeHg exerts slight effects on cell number as visible in the proliferation curves (Fig. 2a). In order to properly quantify the low-dose effects we repeated the proliferation experiment several times. In fact, exposure to 0.03 and 0.30 μM MeHg significantly reduces cell number on day 2 to 92 ± 7 and 88 ± 8% of controls, respectively ($P < 0.05$, respectively). The increasing cell numbers on day 4 and day 6, however, suggest that AFS cells can recover particularly from exposure to 0.03 μM MeHg (Fig. 3a). This raises the question on the involved mechanisms of cytotoxicity and on those able to reverse the effects.

In neuronal cells impressively low MeHg doses (0.0025–0.025 μM) are known to already induce apoptotic cell death via Bax activation, cytochrome C translocation, and caspase and calpain activation and to inhibit cell cycle in G1/S phase (Tamm et al. 2006; Xu et al. 2010). Interestingly, apoptotic-related signals caused by MeHg-induced oxidative stress can be reversed by antioxidants such as *N*-acetylcysteine (NAC), glutathione (GSH), and glycine (Cuello et al. 2010; Lu et al. 2011; Pal et al. 2011). Also the activation of the enzyme Fyn kinase through MeHg-induced oxidative stress (0.02 μM), which finally affects diverse processes among them cell proliferation, survival, and differentiation, is effectively prevented by NAC (Li et al. 2007).

In principle, the protective effect of thiol-containing proteins such as GSH, cysteine, and metallothionein (MT) towards Hg cytotoxicity stems from their high affinity to bind Hg via covalent binding to free sulfhydryl-groups. This binding affinity enables transport into cells in the form of MeHg-cysteine, conjugation to GSH in the cell, and finally its efflux as GSH complex (reviewed in Gundacker et al. 2010). Transporters of the ATP-binding cassette superfamily such as the MRPs (i.e., multidrug resistance-associated proteins 1 and 2) are involved in Hg efflux. Intracellular Hg^{2+} is also retained, first of all by MTs, which are small proteins with unusual high cysteine content confering high metal binding capacity. GSH and MT have a double function in Hg detoxification. As prominent antioxidants they are not only involved in oxidative stress response. Moreover, they confer that MeHg is stably bound (preventing that MeHg binds to critical cellular constituents) and efficiently effluxed from the cell. Because a single mercury atom can bind to and cause the irreversible excretion of up to two GSH tripeptides, MeHg exposure leads to GSH depletion, which must be compensated by regeneration or principally by de novo synthesis (Quig 1998). Accordingly, reversibility of MeHg-induced pro-oxidative effects through GSH or cysteine is limited by endogenous availability of the compounds. In the presence of very high MeHg concentrations and/or long exposure time GSH is depleted and membranes are damaged resulting in necrotic cell death (Cuello et al. 2010). It is known that both reduced Hg accumulation in cells (as the result of slow uptake and rapid efflux) and endogenous GSH levels are major factors mediating resistance towards MeHg (Miura 2000). Support for the assumption that AFS cells can resist low MeHg exposure by increasing Hg efflux comes from our data on Hg accumulation in AFS cells (which is discussed in more detail below). While the cells exposed to 3 μM MeHg continuously accumulate Hg, the Hg levels in AFS cells exposed to 0.3 μM MeHg are decreasing from day 2 down to undetectable levels on day 4 (Fig. 2a). The latter finding can be interpreted in two ways. Either it is a simple dilution effect because AFS cells proliferate further and/or MeHg initiates increased expression of transporter proteins such as the MRPs in order to accelerate Hg efflux.

Taken together, our data indicate that part of AFS cells do not survive 3 μM MeHg treatment, which is very likely caused by apoptotic cell death. It has to be explored whether also G1/S or G2/M cell cycle arrest is involved in the effects of this metal on stem cells. Obviously AFS cell proliferation is less sensitive to MeHg compared with neuronal stem cells and neuronal precursor cells derived from mouse and rat brain tissues (Table 1). A possible explanation for this discrepancy is that neuronal cells are less protected than non-neuronal cell lines because of their lower endogenous GSH levels (Miura 2000). Thus, further experiments are necessary to characterize AFS cells with regard to their antioxidative properties.

The subtle reduction in cell number by low-dose treatment (0.03 μM MeHg) does not necessarily mean that this effect on AFS cell proliferation is biologically irrelevant. Stem cells in amniotic fluid are of fetal origin but the in vivo function of AFS cells in amniotic fluid is still unclear (Rosner et al. 2011). Importantly, it remains to be explored whether pluripotent AFS cells are limited in their differentiation potential in a way that has been already described for murine neural stem cells exposed to a very low MeHg concentration (0.0025 μM). It was clearly indicated in this study that neuronal stem cells are more sensitive to MeHg-induced cytotoxicity than differentiated neurons (Tamm et al. 2006). Similar findings were reported for human embryonic stem cells (hESC), i.e., MeHg seems to inhibit hESC neuronal precursor differentiation by mechanisms different from general cytotoxicity and the differentiation of neuronal precursor-like cells is more sensitive to MeHg exposure than their maturation into neuron-like cells (Stummann et al. 2009). This might be highly relevant also for AFS cells that harbor the potential to differentiate into neurogenic, osteogenic, chondrogenic, adipogenic, hepatic, myogenic, renal, and hematopoietic lineages (Rosner et al. 2011).

Table 1 Selected data on MeHg-induced effects on cell number

Hg species	Dosage (μM)	Time of effect	Cell lineage	Cell number reduction (%)	References
MeHg	0.025	Day 1	Rat embryonic cNSCs (E 15)	80–85	Tamm et al. (2006)
MeHgCl	0.03	Day 2	Rat cerebellar granule neurons (Wistar rat pups)	76	Sakaue et al. (2005)
MeHgCl	0.03	Day 2	Human AFS cells	92	This study
MeHgCl	0.05	Day 4	Rat cerebellar granule cells (Wistar rat pups)	55	Hogberg et al. (2010)
MeHg	0.25	Day 1	Murine neural stem cells (C17.2)	80–85	Tamm et al. (2006)
MeHgCl	0.3	Day 1	Rat cerebellar granule cell precursors (P7 pups)	86	Burke et al. (2006)
MeHgCl	0.3	Day 2	Human AFS cells	88	This study
MeHgCl	0.5	Day 2	Rat cortical progenitor cells (SD embryos E13)	65	Xu et al. (2010)
MeHg	3	Day 1	Murine neuroblastoma cells (Neuro-2a)	40	Lu et al. (2011)
MeHgCl	3	Day 1	Rat cerebellar granule cell precursors (P7 pups)	10	Burke et al. (2006)
MeHgCl	3	Day 1	Rat cortical precursor cells (E14.5 embryos)	25	Burke et al. (2006)
MeHgCl	3	Day 2	Human AFS cells	45	This study
MeHg	4	Day 2	Mouse embryonal fibroblasts (GD 14)	35	Gribble et al. (2005)

Effects of PbAc on cell number of AFS cells

As shown in Figs. 2b and 3b, exposure to 1 μM Pb has no significant effects on the number of AFS cells, neither on days 2, 4 or 6 ($P > 0.05$, respectively), whereas exposure to 10 μM reduces cell number to 92 ± 2% on day 4 ($P < 0.05$). Treatment with 50 μM Pb significantly reduces cell number to 89 ± 6% on day 2 down to 81 ± 5% on day 6 ($P < 0.05$, respectively). As for MeHg it is known that exposure to PbAc influences cell cycle and induces apoptosis. In adult hepatic stem cells exposure to 40 μM PbAc for 6 h reduces cell number to 75%. In this experiment stimulation of caspase cascade and simultaneous ERK dephosphorylation were the most significant pathways associated with Pb-induced apoptotic signals (Agarwal et al. 2009). In PC12 cells it was shown that PbAc can induce DNA damage and apoptosis going along with upregulation of Bax and downregulation of Bcl-2. Additionally, the expression of p53 is increased, and caspase-3 is activated. It was concluded that PbAc can induce activation of p53 by DNA damage, which may lead to imbalance of Bax/Bcl-2 and mitochondrial dysfunction. Subsequently, after activation of caspase-3, Pb-induced cell death occurs (Xu et al. 2006). In normal rat fibroblasts dose-dependent accumulation of cells in the G0/G1 phase was observed, with a compensatory reduction of cells in the S phase. Moreover, Pb exposure from 2.5 to 10 μM was associated with apoptotic cell death up to 20%. Apoptosis decreased at higher Pb concentrations suggesting that at high doses, Pb completely inhibits enzymatic activities, including the ones needed for the induction of apoptotic cell death (Iavicoli et al. 2001).

With regard to cell number reduction, breast cancer cells, adult rat hepatic stem cells, and HepG2 cells appear to respond more sensitive to PbAc exposure than AFS cells (Table 2). Interestingly, PbAc also has a proliferative effect on a variety of cells (rat and mouse kidney, rat liver, vascular smooth muscle, vascular endothelial and spleen cells) (Lu et al. 2002; Zeller et al. 2010). Therefore, it has been assumed that Pb may act as a tumor promoter. The Pb-induced proliferative effect was found to be caused by enhanced DNA synthesis via activation of the MEK1/2 and ERK1/2 signal transduction pathway via a protein kinase C (PKC)-alpha-dependent manner in human astrocytoma cells (Lu et al. 2002).

Our experiments clearly demonstrate antiproliferative effects of PbAc, which, however, occur at concentration greater than 1 μM (200 μg/L). We conclude that Pb concentrations in the physiological range have no adverse effect on the proliferation potential of AFS cells. However, Pb-induced effects on AFS cell differentiation cannot be excluded because other data suggest that even low Pb levels (0.01–10 μM) can affect differentiation of embryonic neural stem cells (Huang and Schneider 2004).

Effects of MeHg and PbAc on cell proliferation are related to Hg and Pb accumulation in cells

We expected that cellular Hg and Pb accumulation is a major factor, which determines the observed dose-dependent changes in cell number and the metal-specific effects on AFS cell proliferation. As has been described earlier for other cell lineages (Bannon et al. 2003; Lewandowski et al. 2003; Aleo et al. 2005), also AFS cells accumulate Hg and Pb in accordance to the dose. We found undetectable Hg and Pb concentrations in cells exposed to 0.03 μM MeHg and 1 μM Pb.

Table 2 Selected data on Pb-induced effects on cell number

Pb species	Dosage (μM)	Time of effect	Cell lineage	Cell number reduction (%)	References
Pb acetate	0.5	Day 2	Rat pheochromocytoma PC12	85	Chen et al. (2003)
Pb	5	Day 2	Human SH-SY5Y neuroblastoma cells	50	Suresh et al. (2006)
Pb acetate	10	Day 4	Human AFS cells	92	This study
Pb chloride	10	Day 4	Rat cerebellar granule cells (Wistar rat pups)	85	Hogberg et al. (2010)
Pb nitrate	15	Day 3	HepG2	50	Tchounwou et al. (2004)
Pb acetate	40	6 h	Adult rat hepatic stem cells	75	Agarwal et al. (2009)
Pb acetate	50	Day 6	Breast cancer MCF-7 cells	53	Corbit et al. (2006)
Pb acetate	50	Day 6	Human AFS cells	81	This study

However, there are three remarkable differences regarding the intracellular accumulation of these two metals:

First, cellular Hg and Pb contents differ substantially in relation to the respective dosages. PbAc was used in much higher (17- to 33-fold higher) concentrations compared with MeHg. However, interestingly the cells accumulate both metals to comparable concentrations. Lower Pb accumulation in AFS cells does well explain the much slighter effects of PbAc on cell proliferation (Figs. 2, 3). One explanation would be that MeHg is more efficiently taken up in cells compared with PbAc. This would somehow be surprising, because both compounds have been described to be highly bio-available in vivo (e.g., Dieter et al. 1993; Clarkson 2002). However, there is evidence that the toxicant's compound and the culture medium together determine the metal speciation and the availability of potential ligands. It is known that MeHg is more efficiently transported into cells, thus more toxic, when complexed with cysteine or homocysteine (Kajiwara et al. 1996; Bridges and Zalups 2005; Yin et al. 2008) and that Pb is cytotoxic when left free in the exposure medium and when complexed with carbonate, cysteine or citrate, but not when complexed with albumin or phosphate (Milgram et al. 2008). In another experiment, the toxic actions of Pb appeared to be inactivated to certain extent by the presence of fetal calf serum (FCS). Progressive reduction in cell number seems to be more evident in cultures with low fetal calf serum (FCS) concentration. The conclusion was that FCS could be capable of fortifying cells against lead-induced cellular damage (Domínguez et al. 2002). Comparable findings were reported for vascular endothelial cells. Under serum-reduced condition Pb is inducing cell death and impairing proliferation, while medium containing serum is stimulating proliferation (Zeller et al. 2010). Other authors stated that FCS is an effective agent for preventing precipitation of Pb from complex media. The increased solubility of Pb in the presence of FCS is likely due to nonspecific binding of Pb to serum proteins such as albumin. Some part of this Pb is available to interact with cellular targets (Mayer and Godwin 2006). In conclusion, the ability of the resulting complexes to serve as substrates for a variety of transporters do greatly influence cellular uptake of the metals, which in turn determines cellular contents and thus the cytotoxicity of the metals. We cultivated AFS cells in Chang C/MEM. So far it remains unknown in which chemical form the here applied Hg and Pb compounds are actually present in this culture medium and thus available to AFS cells. Theoretically, two further mechanisms might play a role in lower Pb accumulation in AFS cells compared with Hg. MT synthesis is known to be induced by both metals. Still, Pb appears to activate MT synthesis with a significant delay compared with Hg (Stacchiotti et al. 2009). Interestingly, in ducks co-exposed to MeHg and PbAc, renal and hepatic MT increased to the same amount as when exposed to each compound alone (Jordan et al. 1990). It remains to be explored whether MT synthesis in human AFS cells respond differently to MeHg and PbAc exposures. A second possibility is that Pb is more rapidly effluxed from AFS cells than Hg. Hitherto it is not known how Pb is effluxed from cells and which proteins are involved. Therefore, it remains to be investigated whether Hg and Pb are differently effluxed from AFS cells, whether PbAc indeed is less efficiently transported into AFS cells than MeHg, and which components in culture medium modulate transport of the metal compounds into AFS cells.

Second, cells exposed to 0.3 μM MeHg and 10 μM PbAc, respectively, showed decreasing cellular Hg content from day 2 to day 4, whereas Pb content increases from day 2 to day 4 (Fig. 2a, b). This accumulation pattern, which we are assuming to be present also in 0.03 μM MeHg and 1 μM PbAc treatments, can explain why proliferation of human AFS cells can recover from low-dose MeHg treatment but not from Pb treatment (Fig. 3a, b). These accumulation patterns do not change when cells are co-exposed to 0.03 μM MeHg and 10 μM Pbac (Fig. 2c).

And last but not least, the high doses (3 μM MeHg, 50 μM Pb) lead to continuous Hg and Pb accumulation with peak contents on day 3 and to comparable or lower contents on day 4, respectively (Fig. 2a, b). In contrast, co-exposed cells accumulate Hg and Pb until day 4, but especially on day 3 Pb content in co-exposed cells is clearly lower compared with cells exposed to Pb alone (Fig. 2c). One potential underlying mechanism for lowered Pb levels in the presence of MeHg might be that MeHg inhibits Pb transporting proteins. There is evidence that divalent metal transporter 1 (DMT1) and Ca-ATPase are involved in cellular Pb uptake (Lidsky and Schneider 2003; Bressler et al. 2004) and that both transporters are markedly inhibited in the presence of Hg (Yallapragada et al. 1996; Marciani et al. 2004). Hg also decreases cadmium (Cd) accumulation by both inhibiting its uptake and enhancing its efflux in rat hepatocytes (Blazka and Shaikh 1992). Cd is also transported by DMT1 (Bressler et al. 2004).

Effects of combined exposure to MeHg and PbAc

The obtained data on proliferation (Figs. 2, 3) and cyclin expression (Fig. 5) indicate that the effects resulting from co-exposure to MeHg and PbAc are the same as for single MeHg treatment. This is confirmed by statistical analysis of cell number and cell size comparing single exposure and co-exposure experiments ($P > 0.05$, respectively). The disappearance of Pb-induced effects on cell proliferation can be explained by the above-discussed cellular contents of Hg and Pb, i.e., the altered accumulation of Pb in AFS cells in the presence of MeHg. However, cells co-exposed to 0.30 μM MeHg and 10 μM PbAc, which also do not show additive effects on cell number, do not display altered Pb accumulation compared with cells treated with Pb alone. To our best knowledge the potential co-exposure effects of MeHg and Pb on cell proliferation and cell size have not been investigated so far in vitro. The available results on animal experiments with mice, rats, and ducks co-exposed to MeHg and PbAc or Pb nitrate brought inconsistent results. According to outcome co-exposure leads to additive, less than additive as well as to synergistic effects (ATSDR 2006).

Conclusions

Human AFS cells exposed to MeHg and PbAc accumulate significantly more Hg than Pb. Accordingly, MeHg-induced effects on cell proliferation are stronger compared with PbAc. Co-exposure to MeHg and PbAc does not have additive effect on proliferation of AFS cells independent of the applied dose. We hypothesize that MeHg is transiently inhibiting cellular Pb intake and/or MeHg induces acceleration of Pb efflux. However, this Pb accumulation pattern does only occur when cells are co-exposed to 3 μM MeHg and 50 μM Pb but not at lower concentrations. Further experiments are necessary to clarify these relationships. Last, under the present experimental conditions, AFS cells appear to be protected against PbAc exposure independent of treatment, i.e., single exposure or combined exposure with MeHg.

Conflict of interest The authors declare that they have no conflict of interest.

References

Agarwal S, Roy S, Ray A, Mazumder S, Bhattacharya S (2009) Arsenic trioxide and lead acetate induce apoptosis in adult rat hepatic stem cells. Cell Biol Toxicol 25(4):403–413

Aleo MF, Morandini F, Bettoni F, Giuliani R, Rovetta F, Steimberg N, Apostoli P, Parrinello G, Mazzoleni G (2005) Endogenous thiols and MRP transporters contribute to Hg^{2+} efflux in $HgCl_2$-treated tubular MDCK cells. Toxicology 206(1):137–151

ATSDR (1999) (United States Agency for Toxic Substances and Disease Registry) Toxicological profile for mercury. http://www.atsdr.cdc.gov/toxprofiles/tp.asp?id=115&tid=24. Accessed 5 Sept 2011

ATSDR (2006) (United States Agency for Toxic Substances and Disease Registry) Interaction profiles for toxic substances. Chlorpyrifos, Lead, Mercury, and Methyl mercury. http://www.atsdr.cdc.gov/interactionprofiles/ip11.html. Accessed 5 Sept 2011

ATSDR (2007) (United States Agency for Toxic Substances and Disease Registry) Toxicological profile for lead. http://www.atsdr.cdc.gov/toxprofiles/tp.asp?id=96&tid=22. Accessed 5 Sept 2011

Bannon DI, Abounader R, Lees PSJ, Bressler JP (2003) Effect of DMT1 knockdown on iron, cadmium, and lead uptake in Caco-2 cells. Am J Physiol Cell Physiol 284(1):C44–C50. doi:10.1152/ajpcell.00184.2002

Blazka ME, Shaikh ZA (1992) Cadmium and mercury accumulation in rat hepatocytes: interactions with other metal ions. Toxicol Appl Pharm 113(1):118–125

Bressler JP, Olivi L, Cheong JH, Kim Y, Bannona D (2004) Divalent metal transporter 1 in lead and cadmium transport. Ann NY Acad Sci 1012:142–152

Bridges CC, Zalups RK (2005) Molecular and ionic mimicry and the transport of toxic metals. Toxicol Appl Pharm 204(3):274–308

Burke K, Cheng Y, Li B et al (2006) Methylmercury elicits rapid inhibition of cell proliferation in the developing brain and decreases cell cycle regulator, cyclin E. NeuroToxicology 27(6):970–981

Chen L, Yang X, Jiao H, Zhao B (2003) Tea catechins protect against lead-induced ROS formation, mitochondrial dysfunction, and calcium dysregulation in PC12 cells. Chem Res Toxicol 16:1155–1161

Clarkson TW (2002) The three modern faces of mercury. Environ Health Perspect 110(S1):11–23

Clarkson TW, Magos L, Myers GJ (2003) The toxicology of mercury: current exposures and clinical manifestations. New Engl J Med 349(18):1731–1737

Corbit R, Ebbs S, King ML, Murphy LL (2006) The influence of lead and arsenite on the inhibition of human breast cancer MCF-7 cell

proliferation by American ginseng root (Panax quinquefolius L.). Life Sci 78(12):1336–1340
Cuello S, Goya L, Madrid Y et al (2010) Molecular mechanisms of methylmercury-induced cell death in human HepG2 cells. Food Chem Toxicol 48(5):1405–1411
Dieter MP, Matthews HB, Jeffcoat RA, Moseman RF (1993) Comparison of lead bioavailability in F344 rats fed lead acetate, lead oxide, lead sulfide, or lead ore concentrate from Skagway, Alaska. J Toxicol Environ Health 39(1):79–93
Domínguez C, Solé E, Fortuny A (2002) In vitro lead-induced cell toxicity and cytoprotective activity of fetal calf serum in human fibroblasts. Mol Cell Biochem 237(1):47–53
EFSA Panel on Contaminants in the Food Chain (CONTAM) (2010) Scientific opinion on lead in food. EFSA J. http://www.efsa.europa.eu/en/efsajournal/pub/1570.htm. Accessed 5 Sept 2011
Falluel-Morel A, Sokolowski K, Sisti HM, Zhou X, Shors TJ, DiCicco-Bloom E (2007) Developmental mercury exposure elicits acute hippocampal cell death, reductions in neurogenesis, and severe learning deficits during puberty. J Neurochem 103(5):1968–1981
Faustman EM, Ponce RA, Ou YC, Mendoza AC, Lewandowski T, Kavanagh T (2002) Investigations of methylmercury-induced alterations in neurogenesis. Environ Health Perspect 110(S5): 859–864
Fingar DC, Salama S, Tsou C, Harlow E, Blenis J (2002) Mammalian cell size is controlled by mTOR and its downstream targets S6K1 and 4EBP1/eIF4E. Gene Dev 16(12):1472–1487
Glahn F, Schmidt-Heck W, Zellmer S et al (2008) Cadmium, cobalt and lead cause stress response, cell cycle deregulation and increased steroid as well as xenobiotic metabolism in primary normal human bronchial epithelial cells which is coordinated by at least nine transcription factors. Arch Toxicol 82(8):513–524
Goyer RA (1990) Transplacental transport of lead. Environ Health Perspect 89:101–105
Grandjean P, Landrigan P (2006) Developmental neurotoxicity of industrial chemicals. Lancet 368(9553):2167–2178
Gribble EJ, Hong SW, Faustman EM (2005) The magnitude of methylmercury-induced cytotoxicity and cell cycle arrest is p53-dependent. Birth Defects Res A 73(1):29–38
Gundacker C, Gencik M, Hengstschläger M (2010) The relevance of the individual genetic background for the toxicokinetics of two significant neurodevelopmental toxicants: Mercury and lead. Mutat Res-Rev Mutat 705(2):130–140
Hogberg HT, Kinsner-Ovaskainen A, Coecke S, Hartung T, Bal-Price AK (2010) mRNA expression is a relevant tool to identify developmental neurotoxicants using an in vitro approach. Toxicol Sci 113(1):95–115
Huang F, Schneider JS (2004) Effects of lead exposure on proliferation and differentiation of neural stem cells derived from different regions of embryonic rat brain. NeuroToxicology 25(6):1001–1012
Iavicoli I, Sgambato A, Carelli G, Ardito R, Cittadini A, Castellino N (2001) Lead-related effects on rat fibroblasts. Mol Cell Biochem 222(1):35–40
Jordan SA, Bhatnagar MK, Bettger WJ (1990) Combined effects of methylmercury, lead, and cadmium on hepatic metallothionein and metal concentrations in the pekin duck. Arch Environ Con Tox 19(6):886–891
Kajiwara Y, Yasutake A, Adachi T, Hirayama K (1996) Methylmercury transport across the placenta via neutral amino acid carrier. Arch Toxicol 70(5):310–314
Kalaszczynska I, Geng Y, Iino T, Mizuno S, Choi Y, Kondratiuk I, Silver DP, Wolgemuth DJ, Akashi K, Sicinski P (2009) Cyclin A is redundant in fibroblasts but essential in hematopoietic and embryonic stem cells. Cell 138:352–365
Lewandowski TA, Ponce RA, Charleston JS, Hong S, Faustman EM (2003) Effect of methylmercury on midbrain cell proliferation during organogenesis: potential cross-species differences and implications for risk assessment. Toxicol Sci 75(1):124–133
Li Z, Dong T, Pröschel C, Noble M (2007) Chemically diverse toxicants converge on Fyn and c-Cbl to disrupt precursor cell function. PLoS Biol 5(2):e35. doi:10.1371/journal.pbio.0050035
Lidsky TI, Schneider JS (2003) Lead neurotoxicity in children: basic mechanisms and clinical correlates. Brain 126(1):5–19
Lu H, Guizzetti M, Costa LG (2002) Inorganic lead activates the mitogen-activated protein kinase kinase-mitogen-activated protein kinase-p90RSK signaling pathway in human astrocytoma cells via a protein kinase C-dependent mechanism. J Pharmacol Exp Ther 300(3):818–823
Lu TH, Hsieh SY, Yen CC et al (2011) Involvement of oxidative stress-mediated ERK1/2 and p38 activation regulated mitochondria-dependent apoptotic signals in methylmercury-induced neuronal cell injury. Toxicol Lett 204(1):71–80
Marciani P, Trotti D, Hediger MA, Monticelli G (2004) Modulation of DMT1 activity by redox compounds. J Membrane Biol 197(2):91–99
Mayer RA, Godwin HA (2006) Preparation of media and buffers with soluble lead. Anal Biochem 356(1):142–144
Milgram S, Carrière M, Thiebault C, Malaval L, Gouget B (2008) Cytotoxic and phenotypic effects of uranium and lead on osteoblastic cells are highly dependent on metal speciation. Toxicology 250(1):62–69
Miura K (2000) Methylmercury toxicity at cellular levels–From growth inhibition to apoptotic cell death. J Health Sci 46(3): 182–186
Pal P, Pal S, Das J, Sil P (2011) Modulation of mercury-induced mitochondria-dependent apoptosis by glycine in hepatocytes. Amino Acids. doi:10.1007/s00726-011-0869-3
Papanikolaou NC, Hatzidaki EG, Belivanis S, Tzanakakis GN, Tsatsakis AM (2005) Lead toxicity update: a brief review. Med Sci Monit 11:329–336
Quig D (1998) Cysteine metabolism and metal toxicity. Altern Med Rev 3(4):262–270
Rice D, Barone S (2000) Critical periods of vulnerability for the developing nervous system: evidence from humans and animal models. Environ Health Perspect 108(S3):511–533
Rosner M, Mikula M, Preitschopf A, Feichtinger M, Schipany K, Hengstschläger M (2011) Neurogenic differentiation of amniotic fluid stem cells. Amino Acids. doi:10.1007/s00726-011-0929-8 (in press)
Sakaue M, Okazaki M, Hara S (2005) Very low levels of methylmercury induce cell death of cultured rat cerebellar neurons via calpain activation. Toxicology 213(1–2):97–106
Stacchiotti A, Morandini F, Bettoni F, Schena I, Lavazza A, Grigolato PG, Apostoli P, Rezzani R, Aleo MF (2009) Stress proteins and oxidative damage in a renal derived cell line exposed to inorganic mercury and lead. Toxicology 264(3):215–224
Stern AH, Smith AE (2003) An assessment of the cord blood:maternal blood methylmercury ratio: implications for risk assessment. Environ Health Perspect 111(12):1465–1470
Stummann TC, Hareng L, Bremer S (2009) Hazard assessment of methylmercury toxicity to neuronal induction in embryogenesis using human embryonic stem cells. Toxicology 257(3):117–126
Suresh C, Dennis AO, Heinz J, Vemuri MC, Chetty CS (2006) Melatonin protection against lead-induced changes in human neuroblastoma cell cultures. Int J Toxicol 25(6):459–464
Tamm C, Duckworth J, Hermanson O, Ceccatelli S (2006) High susceptibility of neural stem cells to methylmercury toxicity: effects on cell survival and neuronal differentiation. J Neurochem 97(1):69–78

Tchounwou PB, Yedjou CG, Foxx DN, Ishaque AB, Shen E (2004) Lead-induced cytotoxicity and transcriptional activation of stress genes in human liver carcinoma (HepG2) cells. Mol Cell Biochem 255(1):161–170

Valli A, Rosner M, Fuchs C, Siegel N, Bishop CE, Dolznig H, Madel U, Feichtinger W, Atala A, Hengstschlager M (2010) Embryoid body formation of human amniotic fluid stem cells depends on mTOR. Oncogene 29(7):966–977

Wigle DT, Lanphear BP (2005) Human health risks from low-level environmental exposures: no apparent safety thresholds. PLoS Med 2(12):e350. doi:10.1371/journal.pmed.0020350

Xu J, Ji LD, Xu LH (2006) Lead-induced apoptosis in PC 12 cells: Involvement of p53, Bcl-2 family and caspase-3. Toxicol Lett 166(2):160–167

Xu M, Yan C, Tian Y, Yuan X, Shen X (2010) Effects of low level of methylmercury on proliferation of cortical progenitor cells. Brain Res 1359:272–280

Yallapragada PR, Rajanna S, Fail S, Rajanna B (1996) Inhibition of calcium transport by mercury salts in rat cerebellum and cerebral cortex in vitro. J Appl Toxicol 16(4):325–330

Yin Z, Jiang H, Syversen T, Rocha JBT, Farina M, Aschner M (2008) The methylmercury-L-cysteine conjugate is a substrate for the L-type large neutral amino acid transporter. J Neurochem 107(4):1083–1090

Zeller I, Knoflach M, Seubert A et al (2010) Lead contributes to arterial intimal hyperplasia through nuclear factor erythroid 2-related factor-mediated endothelial interleukin 8 synthesis and subsequent invasion of smooth muscle cells. Arterioscl Throm Vas 30(9):1733–1740